Journal of Applied Electrochemistry (2019) 49:839–846
https://doi.org/10.1007/s10800-019-01326-x

SHORT COMMUNICATION

Au nanodendrite incorporated graphite pencil lead as a sensitive and simple electrochemical sensor for simultaneous detection of Pb(II), Cu(II) and Hg(II)

Nguyen Quynh Giao[1] · Vu Hai Dang[1] · Pham Thi Hai Yen[1] · Pham Hong Phong[1] · Vu Thi Thu Ha[1,2] · Pham Khac Duy[3,4] · Hoeil Chung[4]

Received: 1 March 2019 / Accepted: 5 June 2019 / Published online: 17 June 2019

Abstract

Graphite pencil lead (GPL) covered with Au nanodendrites (AuNDs) (the AuND@GPL sensor) has been demonstrated as an electrochemical sensor for simultaneous detection of Pb(II), Cu(II) and Hg(II) in water samples. To meet both the demands of cost-effectiveness and required analytical performance, a cheap GPL was chosen as a sensor platform and AuNDs providing a large electroactive surface area were fabricated on the surface of GPL by a simple electrodeposition in less than one minute. Due to the incorporation of AuNDs, the sensitivities of simultaneous detection of Pb(II), Cu(II) and Hg(II) were improved with a limit of detection below 0.2 ppb, and the peak intensities did not vary significantly even though concentrations of interferants were 100-fold greater. The sensor-to-sensor reproducibility was good (relative standard deviation below 4.6%), which is mainly contributed to the simple one-step electrodeposition for sensor preparation. The overall detection performance was better or similar in comparison with those of previously reported GPL-based sensors. Moreover, when real lake water samples were analyzed, the AuND@GPL sensor was able to accurately determine the Pb(II), Cu(II) and Hg(II) concentrations. The sensor is cost-effective due to the use of GPL as a platform, so it has a strong potential as a disposable electrochemical sensor for at-site water quality monitoring.

Graphic abstract

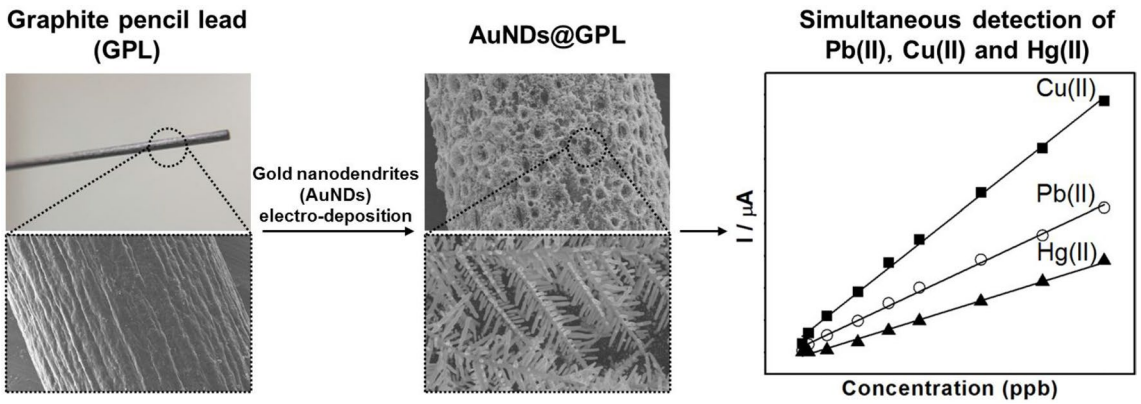

Keywords Graphite pencil lead · Au nanodendrites · Disposable electrochemical sensor · Heavy metal ion detection · Multi-metal detection

✉ Vu Thi Thu Ha
havt@ich.vast.vn

Extended author information available on the last page of the article

1 Introduction

The carbon-based material has been widely utilized for electrochemical sensor because of its unique electronic, mechanical, and chemical properties [1–4]. Among these, GPL has been a very attractive conducting material for use as an electrochemical sensing platform since it is cheap, easily obtainable, and consistent in shape and quality [5, 6]. Based on these merits, diverse GPL-incorporated electrochemical sensors have been developed for detection of various toxic heavy metal ions in water, as summarized in Table 1. Electrochemically superior materials, such as bismuth film [7–10], polystyrene sulfonate–carbon nanopowder [11], nafion–graphene nanocomposites [12], polyaniline film doped with copper-carmoisine dye [13], and reduced graphene oxide [14] were introduced on GPL for the preparation of sensors to achieve desired detection performances in each study. As shown, the achieved limit of detections (LODs) were quite low to be applicable for practical field analysis; nonetheless, there is a continuing demand for a more sensitive, rugged, and simply preparable GPL-based sensor. Actually, more than two fabrication steps were required in the preparation of the listed GPL-based sensors.

As a part of the efforts in exploring GPL-based sensors, our group previously reported a mechanical pencil lead (MPL)-supported carbon nanotube (CNT)/Au nanodendrite sensor and demonstrated its performance for the detection of As(III) [15]. The nanodendrite structure was able to ensure sensitivity since its structure was hierarchical with a high population of edges, thereby providing much large electrochemically active surface area. It is noteworthy that the co-deposition of CNTs and Au on MPL was fairly difficult to control due to CNT aggregation during the process, so sensor-to-sensor reproducibility would degrade. Further, only a single heavy metal ion rather than multiple metal ions was measured. The ability to simultaneously measure multiple metal ions is greatly beneficial to enhancing the analytical utility of the sensor.

This study has aimed to develop a very simple AuNDs-covered GPL sensor (the AuND@GPL sensor), in which AuNDs structure were fabricated on GPL by a one-step electrodeposition in less than 1 min without further incorporation of CNTs. The AuND@GPL sensor was utilized to simultaneously measure three common toxic heavy metal ions [Pb(II), Cu(II), and Hg(II)]. Six AuND@GPL sensors were separately prepared and resulting electrochemical signals were analyzed to assess the sensor-to-sensor reproducibility, response range, and LODs. Next, the selectivity of measurement was tested by preparing samples containing interferants, with concentrations 100-fold greater than the target analyte concentrations and the resulting electrochemical signals of the samples were examined. Finally, to

Table 1 Descriptions of previously reported GPL-based sensors and their achieved LODs

Incorporated materials with GPL	Detected metal	LOD (ppb)	Linear range (ppb)	References
Pencil-lead Bismuth film	Cd, Pb, Zn	Cd: 0.3, Pb: 0.4, Zn: 0.4	2 ÷ 24	[7]
Pencil-lead Bismuth film	Pb	Not given	Not given	[8]
Pencil-lead Bismuth film	Zn, Cd, Pb, Cu	Not given	Zn: 80 ÷ 380 Cd: 5 ÷ 11 Pb: 20 ÷ 65 Cu: 30 ÷ 60	[9]
Bismuth-modified graphite pencil	Pb, Cd, Zn	Cd: 1.0, Pb: 2.0, Zn: 5.0	3 ÷ 50	[10]
PSS–CnP/PGE[a]	Cu	0.11	0 ÷ 210	[11]
NG-PG-BiE[b]	Zn, Cd, Pb	Zn: 0.17, Cd: 0.09, Pb: 0.13 (for individual) Zn: 0.22, Cd: 0.10, Pb: 0.18 (for simultaneous)	2 ÷ 20 10 ÷ 100	[12]
PGE/PA/Cu-Car[c]	Cu	128	$320 \div 64 \times 10^5$	[13]
ERGO-PG-BiE[d]	Zn, Cd, Pb	Zn: 0.19, Cd: 0.09, Pb: 0.12 (for individual) Zn: 0.25, Cd: 0.10, Pb: 0.13 (for simultaneous)	10 ÷ 100	[14]
MPL-CNT/AuNDs[e]	As	0.40	0.5 ÷ 80	[15]

[a]Polystyrene sulfonate–carbon nanopowders modified pencil graphite electrode (PGE)

[b]Nafion graphene nanocomposite pencil graphite bismuth-film electrode

[c]Polyaniline-conducting polymer film doped with copper carmoisine dye complex coated on PGE

[d]Electrochemically reduced graphene oxide pencil graphite bismuth-film electrode

[e]Mechanical pencil lead-supported carbon nanotube/Au nanodendrites electrode

demonstrate practical usage of the sensor, Pb(II), Cu(II) and Hg(II) concentrations from lake water samples in Hanoi, Vietnam, were determined using a standard addition method and subsequent accuracies were evaluated.

2 Experimental section

The reagents used in this study were of analytical grade and used without further purification. Standard Pb(II), Cu(II) and Hg(II) solutions (1000 ppm, atomic absorption standards) were purchased from Merck company (USA). All reagents necessary for construction of AuNDs [$HAuCl_4$ (99.999%), KI, H_2SO_4, and NH_4Cl] were obtained from Sigma-Aldrich. GPL (Dong-A XQ Ceramics, B type, 0.5 mm diameter, and 70 mm length) was purchased at a local office supply store. The GPL was cut to a length of 30 mm and one end was connected to a Cu wire for electrical contact. Since a B-type pencil lead contains a large amount of clay and wax on the surface (approximately 30%), adhesion of AuNDs on the surface would not be facile [11]. Therefore, the wax coating was removed by gently polishing the surface of the GPL using 3000 grit abrasive paper and the polished GPL was subject to sonication in an acetone and nitric acid solution over 15 min.

Initially, electrochemical activation of GPL was accomplished by applying a potential of − 1.5 V (vs. Ag/AgCl) in 0.5 M H_2SO_4 over 300 s. Then the 30 mm length of GPL was kept in Teflon body, only 10 mm of GPL was protruded (image not shown). The activated GPL (only a part of 10 mm) was immersed in a solution containing 20 mM $HAuCl_4$, 1 mM KI, 5 M NH_4Cl, and 0.5 M H_2SO_4, then AuNDs were constructed on the GPL surface by a galvanostatic technique. In fact, the galvanic current for AuNDs deposition was studied and optimized by varying applied current from − 10 to − 70 mA. Data collected showed that by application of − 50 mA (315 mA cm^{-2}) over 30 s, the best signals of Pb(II), Cu(II) and Hg(II) samples were recorded. The potential adopted during the galvanic experiment was in the range from − 2.8 V to − 2.6 V. The constructed AuND@GPL sensor was gently cleaned with acetone and distilled water. All electrochemical measurements were carried out at room temperature (25 °C ± 2) using a potentiostat (PGSTAT 302, Metrohm-Autolab, The Netherlands) equipped with a conventional three-electrode system including Ag/AgCl as a reference electrode and Pt wire as a counter electrode. Scanning electron microscope (SEM) images of the AuNDs structure were obtained using a Hitachi S-4800 SEM instrument. ICP-MS (Perkin Elmer Elan 9000) was used for data comparison.

Pb(II), Cu(II) and Hg(II) samples with various concentrations were prepared by diluting each standard solution. For differential pulse anodic stripping voltammetry (DPASV) measurement, a differential step of 5 mV, a modulation time of 0.03 s, an interval time of 0.08 s, and a modulation amplitude of 50 mV were employed. A 0.1 M KCl/HCl solution (pH = 1) was used as a supporting electrolyte in all measurements. Voltammograms for mixture samples of Pb(II), Cu(II) and Hg(II) were recorded over a range from − 0.3 to + 0.7 V. All potentials given in this research were with respect to the Ag/AgCl reference electrode. Real water samples were collected from West Lake, Hanoi, Vietnam. Initially, 500 mL of the lake water was filtered through a Whatman glass fiber filter (45 µm) in order to remove potential suspended particulates. Then HNO_3 was added to the filtered water until its pH reached 1.0. The treated lake water samples were stored in a dark environment before actual measurement.

3 Results and discussion

Figure 1 shows SEM images of original GPL (a), polished GPL (p-GPL) (b) using 3000 grit abrasive and electrochemical treated p-GPL (c) (by applying a potential of − 1.5 V (vs. Ag/AgCl) in 0.5 M H_2SO_4 over 300 s mentioned above) as below for comparison.

As shown, the wax plating was removed after polishing step and the p-GPL surface became more homogeneous. Intentionally at the first step (a, b), we physically removed the hydrophobic wax layer on GPL surface to induce the interaction of GPL with electrolyte. In the next step (b, c), the wax clusters locating between graphite particles were electrochemically dissolved in order to maximize the conductivity of GPL platform and ease the AuNDs deposition step. Because of preparation steps were carried out under gently polishing and electrochemical treatment, it is believed that the wax coating was effectively removed from GPL surface and GPL shape was kept consistently.

Figure 2 shows SEM images of constructed AuNDs on GPL with 30-s electrodeposition. In the large field of view (Fig. 2a), the pores generated by hydrogen bubbles from the reduction of hydronium ions are apparent and their sizes range from 20 to 40 µm in diameter. In the magnified view (Fig. 2b), the typical shape of dendritic structure with well-aligned terraces is clear, and no aggregation or agglomeration of AuNDs is observed. The pores allow easy internal access of analytes to the Au surface for electrochemical reaction and the large surface area of AuNDs is advantageous, eventually leading to enhanced detection sensitivity. Figure 2c shows cyclic voltammograms (CVs) of 5 mM $K_3Fe(CN)_6$ measured using a bare GPL and AuND@GPL sensor at a scan rate of 0.1 V s^{-1}. The anodic and cathodic peaks are observed in both cases; while, the intensities are higher with the use of the AuND@GPL sensor, indicating the increased current density by the introduced AuNDs.

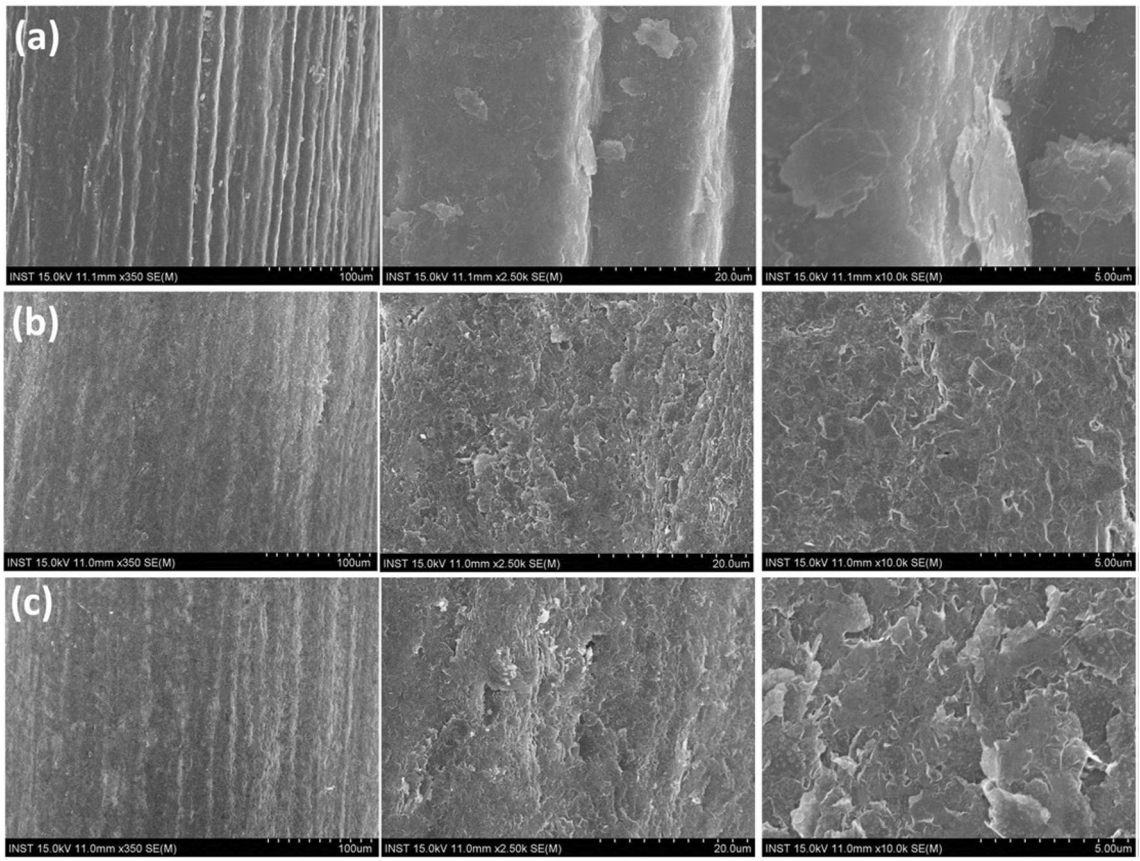

Fig. 1 SEM images of original GPL (**a**), polished GPL (p-GPL) (**b**) using 3000 grit abrasive and electrochemical treated p-GPL (**c**)

Next, by changing the scan rate from 0.01 to 0.4 V s^{-1}, the relationship between peak current (i_p) and the square root of scan rate ($\nu^{1/2}$) in the case of using the AuND@GPL sensor was investigated (refer to Fig. 2d). The relationship was highly linear ($R^2 = 0.9996$, refer to the inset), thereby indicating the reversible redox process in the tested scan rate range.

As presented in authors' publication [16], the area of electrochemical activity of AuNDs developed on GPL as calculated based on Randles–Sevcik equation: $i_p = 2.69 \times 10^5 n^{3/2} D^{1/2} A_{active} C v^{1/2}$, where $C = 5 \times 10^{-6}$ mol cm^{-3}, $v = 100$ mV s^{-1}, $D = 7.5 \times 10^{-6}$ cm^2 s^{-1} [17], active surface areas (ESA) of AuNDs received after 30 s of deposition on GPL electrode ($d = 0.05$ cm, $l = 1.0$ cm) are about 0.173 cm^2. It means that ESA reaches up to 2.40 times higher than that activated area before AuNDs deposition (about 0.072 cm^2). It was initially necessary to confirm the presence of individual Pb(II), Cu(II) and Hg(II) peaks and also potential overlap among the peaks, which degrade the accuracy of quantitative analysis. The inset in Fig. 3 shows DPASV (Differential pulse anodic stripping voltammetry) response of a 0.1 M KCl/HCl solution (pH = 1) solution containing 20 ppb each of Pb(II), Cu(II) and Hg(II). The pre-concentration time was 60 s. As shown, the Pb(II) peak at − 0.08, the Cu(II) peak at 0.37, and the Hg(II) peak at 0.52 V are apparent, and these peaks are nearly free of overlap. In the DPSAV measurement, pre-concentration time related to the amount of enriched analyte at the surface also governs sensitivity. For investigation, the same 20 ppb sample was measured by changing the pre-concentration time from 60 to 600 s (increments of 60 s) and the resulting variations of peak intensities were analyzed as shown in Fig. 3. The intensities of Pb(II) and Hg(II) gradually increased up to the pre-concentration time of 300 s and no noticeable enhancements after 300 s were observed; while, the intensity of the Cu(II) peak continually rose until 600 s. By considering the increasing trends together, 300 s was chosen as the pre-concentration time for subsequent experiments.

To evaluate the advantage of AuNDs in electrochemical measurement, GPL modified with gold nanoparticles (AuNPs@GPL) and unmodified GPL were used to measure sample contained 20 ppb of Pb(II), Cu(II) and Hg(II). As a result, Fig. 4 presents the DPASV response of AuNDs@GPE (dash-dotted), AuNPs@GPE (dotted), and GPE only (solid line) for 20 ppb each of Pb(II), Cu(II) and Hg(II) in 0.1 M KCl/HCl solution at pH = 1. When the accumulation process was carried out for 300 s at − 0.3 V followed by an

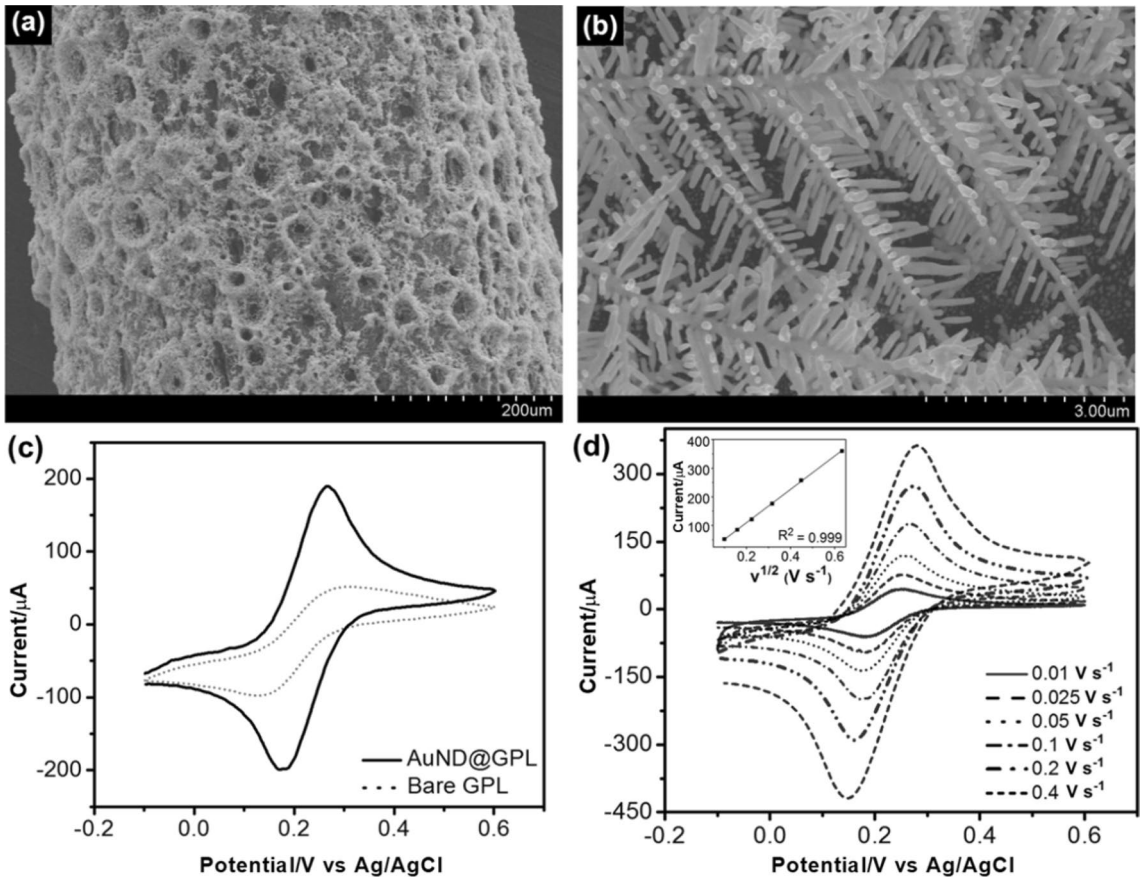

Fig. 2 SEMs images of AuND@GPL with different fields of view (**a**) and (**b**); CVs of 5 mM $K_3Fe(CN)_6$/0.1 M phosphate buffer obtained using AuND@GPL (solid line) and bare GPL (dotted line) with a scan rate of 0.1 V s^{-1} (**c**); CVs of 5 mM $K_3Fe(CN)_6$/0.1 M phosphate buffer obtained using the AuND@GPL with different scan rates (**d**) and the relationship between peak current (i_p) and the square root of the scan rate ($\nu^{1/2}$) is shown in the inset

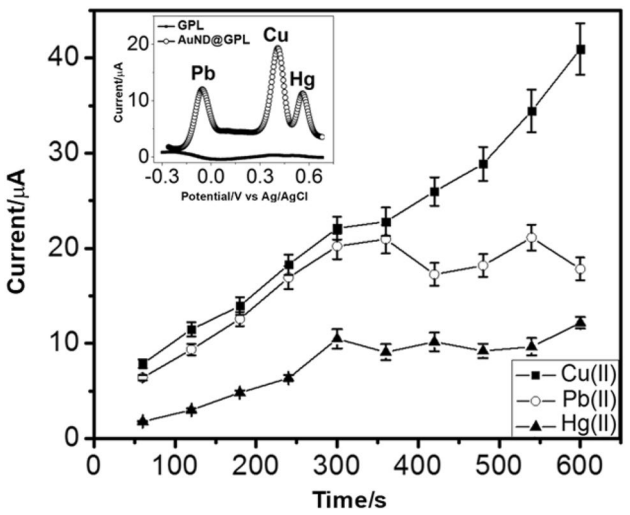

Fig. 3 Variation of peak intensities of Pb(II), Cu(II) and Hg(II) when the pre-concentration time changes from 60 to 600 s (increments of 60 s). The inset shows DPASV responses of Pb(II), Cu(II) and Hg(II) when bare GPL and AuND@GPL sensors are used for measurement

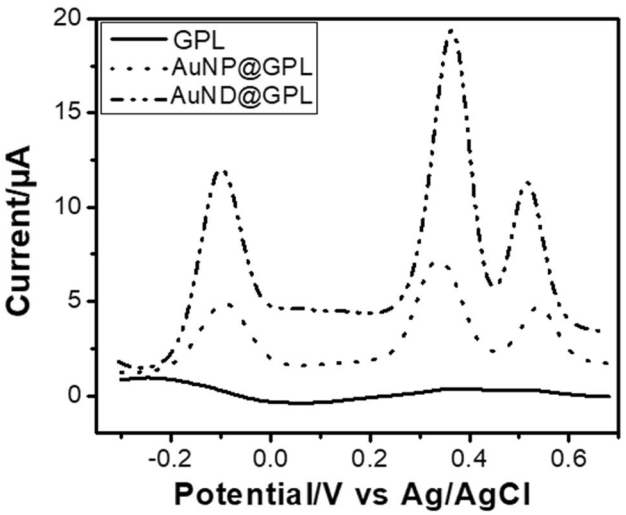

Fig. 4 DPASV response of AuND@GPL (dash-dotted line), AuNPs@GPL (dotted line), and GPL only (solid line) for 20 ppb each of Pb(II), Cu(II) and Hg(II) in 0.1 M KCl/HCl solution at pH = 1

anodic scan from −0.3 to 0.7 V, the peak currents for three target metal ions were acquired with good signal-to-noise ratio. The peaks of Pb(II), Cu(II) and Hg(II) acquired by AuND@GPL were approximately 2 and 5 times higher than that obtained by AuNPs@GPL and GPL only, respectively.

To evaluate the sensitivity, nine samples containing Pb(II), Cu(II) and Hg(II) in the concentration range from 1 to 50 ppb were measured using the AuND@GPL sensor and acquired voltammograms were analyzed (Fig. 5a). The intensities of all Pb(II), Cu(II) and Hg(II) peaks individually increase with the elevation of concentrations, where the Cu peak varies most sensitively. As pH of study solutions chosen is 1, metal stripping peaks become increasingly sharper as indicated in [18], acid dissociation constant ($-\log K_a$) for aqueous metal ion:

$$M^{n+} + H_2O \overset{K_a}{\leftrightarrow} MOH^{(n-1)} + H^+$$

It is in agreement with previous publications [19, 20].

Figure 5b shows the intensities of the Pb(II) peak at −0.08, the Cu(II) peak at 0.37, and the Hg(II) peak at 0.52 V according to the concentration change. For all three analytes, the responses are linear over the tested concentration range ($R^2 > 0.995$) and the slope is steepest in the measurement of Cu(II) as expected. It is necessary to note that the error bars in this figure were based on the independent measurements using six separately prepared AuND@GPL sensors. The average relative standard deviations (RSDs) of Pb(II), Cu(II) and Hg(II) peak intensities were 3.7, 4.6, and 4.3%, respectively. This result confirms the superior sensor-to-sensor reproducibility that is most probably contributed by the simple one-step electrodeposition for sensor preparation. Besides, the repeatability was estimated using five successive measurements on one sensor, the relative standard deviations (RSDs) of Pb(II), Cu(II) and Hg(II) are also < 5%. These results indicated superior stability of proposed AuND@GPL sensor. The LODs in the measurements of Pb(II), Cu(II) and Hg(II) were 0.12, 0.19, and 0.18 ppb, respectively. Compared to those of previous studies in Table 1, the achieved LODs are lower or comparable.

Next, selectivity of the measurements was evaluated by adding interferants [Zn(II), Fe_{total}(II/III), Mn(II), Mg(II), Ni(II), Cr(III), and Ca(II)] into a sample containing 10 ppb of Pb(II), Cu(II) and Hg(II) and then analyzing the changes of the peak intensities relative to those obtained from a sample without the interferants. The concentrations of added

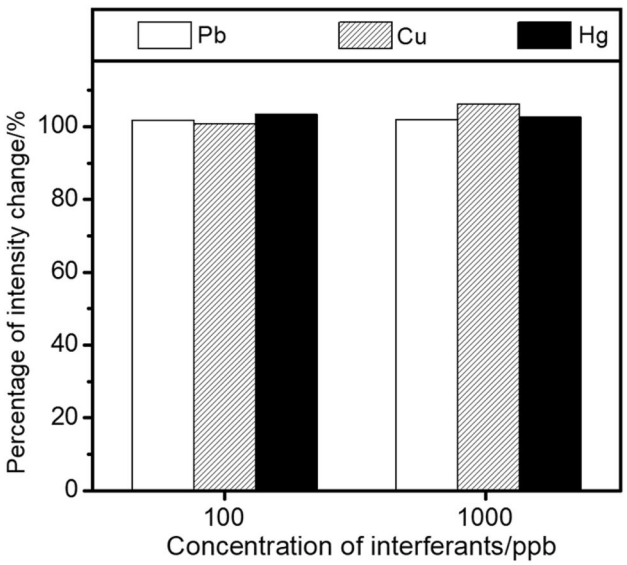

Fig. 6 Percentages of intensity variations of Pb(II), Cu(II), and Hg(II) peaks when the added interferant concentrations are 100 and 1000 ppb

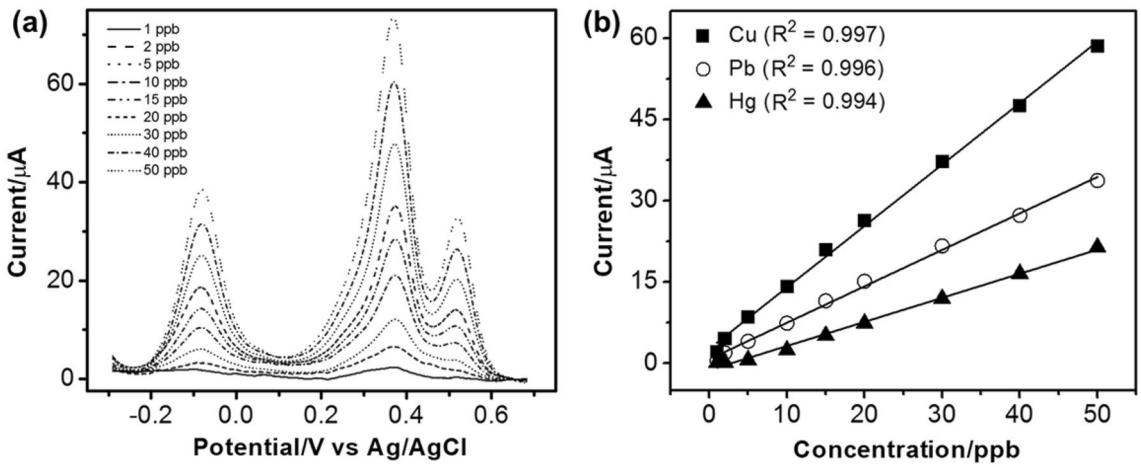

Fig. 5 Voltammograms acquired from 9 mixture samples of Pb(II), Cu(II) and Hg(II) in the concentration range from 1 to 50 ppb (**a**) and the variations of peak intensities according to the concentration change (**b**)

Table 2 Determined Pb(II), Cu(II) and Hg(II) concentrations in real lake water samples by a standard addition method and the corresponding recoveries in comparison with ICP-MS

C (ppb)	Method	Pb(II)		Cu(II)		Hg(II)	
		Caculated (ppb)	Recovery (%)	Caculated (ppb)	Recovery (%)	Caculated (ppb)	Recovery (%)
5.00	DPASV	4.96 ± 0.21	99.20 ± 4.20	4.94 ± 0.18	98.8 ± 3.60	5.17 ± 0.25	103.4 ± 5.00
	ICP-MS	4.68 ± 0.12	93.60 ± 2.40	4.74 ± 0.16	94.8 ± 3.20	4.61 ± 0.17	92.2 ± 3.40
10.00	DPASV	10.65 ± 0.28	106.50 ± 2.80	10.09 ± 0.23	100.9 ± 4.60	9.87 ± 0.31	98.7 ± 3.10
	ICP-MS	9.43 ± 0.18	94.30 ± 1.80	9.62 ± 0.21	96.20 ± 2.1	9.38 ± 0.25	93.80 ± 2.5
15.00	DPASV	15.13 ± 0.32	100.87 ± 2.13	14.82 ± 0.26	98.8 ± 1.73	14.74 ± 0.38	98.27 ± 2.53
	ICP-MS	14.47 ± 0.27	96.47 ± 1.80	14.39 ± 0.22	95.93 ± 1.47	14.46 ± 0.19	96.40 ± 1.27

interferants were 100 and 1000 ppb. Figure 6 shows the percentages of peak intensity variations under the interferant concentrations of 100 and 1000 ppb, which were calculated following the equation given in recently published paper of the author group [16]:

$$\frac{I_p^{Me}(Pb, Cu, Hg) * 100}{I_p^0(Pb, Cu, Hg)}(\%)$$

$I_p^{Me}(Pb, Cu, Hg)$ is peak height of Pb(II), Cu(II) and Hg(II) in solution containing interferants. $I_p^0(Pb, Cu, Hg)$ is peak height of Pb(II), Cu(II) and Hg(II) in solution without interferants. One hundred percent (100%) implies no interference. As shown, no considerable interferences were observed in the measurements of Pb(II), Cu(II) and Hg(II), even though the interferant concentration was 100-fold greater than those of the target heavy metal ions. It can be explained that those metals has reduction potential differently from target metals, for example, − 1.0 V for Fe(II) [21], − 1.35 V and − 0.9 V for Mn(II) and Zn(II) [22], respectively. Finally, the AuND@GPL sensor was employed to measure Pb(II), Cu(II) and Hg(II) concentrations in water samples collected from West Lake, Hanoi, Vietnam. A standard addition method was used to determine the concentrations. The determined concentrations of each of the heavy metal ions and the corresponding recoveries are presented in Table 2. Based on the observation, the proposed sensor was able to accurately determine the Pb(II), Cu(II) and Hg(II) concentrations in real field water samples.

4 Conclusions

The analytical performances of the AuND@GPL sensor such as sensitivity, selectivity, and sensor-to-sensor reproducibility are acceptable to be employed for simultaneous detection of Pb(II), Cu(II) and Hg(II) in real samples. The most practical advantage of the AuND@GPL sensor was the simple fabrication in less than 1 min. Moreover, the sensor is cost-effective due to the use of GPL as a platform, so it has strong potential as a disposable electrochemical sensor for at-site water quality monitoring. Currently, a portable measurement system incorporating AuND@GPL as a disposable sensor is under development as a part of a mobile water quality-monitoring station.

Acknowledgements This research is funded by Vietnam National Foundation for Science and Technology Development (NAFOSTED) under Grant Number 104.06-2016.25.

References

1. Gan T, Hu C, Hu S (2014) Preparation of graphene oxide–fullerene/phosphotungstic acid films and their application as sensor for the determination of cis-jasmone. Anal Methods 6:9220–9227
2. Gan T, Hu C, Chen Z (2011) Novel electrocatalytic system for the oxidation of methyl jasmonate based on layer-by-layer assembling of montmorillonite and phosphotungstic acid nanohybrid on graphite electrode. Electrochim Acta 56:4512–4517
3. Gan T, Hu C, Chen Z, Hu S (2010) Fabrication and application of a novel plant hormone sensor for the determination of methyl jasmonate based on self-assembling of phosphotungstic acid–graphene oxide nanohybrid on graphite electrode. Sens Actuators, B 151:8–14
4. Gan T, Hu C, Chen Z, Hu S (2011) A disposable electrochemical sensor for the determination of indole-3-acetic acid based on poly(safranine T)-reduced graphene oxide nanocomposite. Talanta 85:310–316
5. Kawde AN, Baig N, Sajid M (2016) Graphite pencil electrodes as electrochemical sensors for environmental analysis: a review of features, developments, and applications. RSC Adv 6:91325–91340
6. David IG, Popa DE, Buleandra M (2017) Pencil graphite electrodes: a versatile tool in electroanalysis. J Anal Methods Chem. https://doi.org/10.1155/2017/1905968
7. Demetriades D, Economou A, Voulgaropoulos A (2004) A study of pencil-lead bismuth-film electrodes for the determination of trace metals by anodic stripping voltammetry. Anal Chim Acta 519:167–172
8. Goldcamp MJ, Underwood MN, Cloud JL, Harshman S (2008) An environmentally friendly, cost-effective determination of lead in environmental samples using anodic stripping voltammetry. J Chem Educ 85:976–979
9. Pierini GD, Pistonesi MF, Nezio MSD, Centurión ME (2016) A pencil-lead bismuth film electrode and chemometrics tools for

simultaneous determination of heavy metals in propolis samples. Microchem J 125:266–272
10. Kawde AN (2016) Electroanalytical determination of heavy metals in drinking waters in the eastern province of Saudi Arabia. Desalin Water Treat 57:15697–15705
11. Cantalapiedra A, Gismera MJ, Procopio JR, Sevilla MT (2015) Electrochemical sensor based on polystyrene sulfonate–carbon nanopowders composite for Cu (II) determination. Talanta 139:111–116
12. Pokpas K, Jahed N, Tovide O, Baker PG, Iwuoha EI (2014) Nafion-graphene nanocomposite in situ plated bismuth-film electrodes on pencil graphite substrates for the determination of trace heavy metals by anodic stripping voltammetry. Int J Electrochem Sci 9:5092–5115
13. Ansari R, Delavar AF, Aliakbar A, Mohammad-khar A (2012) Solid-state Cu (II) ion-selective electrode based on polyaniline-conducting polymer film doped with copper carmoisine dye complex. J Solid State Electrochem 16:869–875
14. Pokpas K, Zbeda S, Jahed N, Mohamed N, Baker PG, Iwuoha EI (2014) Electrochemically reduced graphene oxide pencil-graphite in situ plated bismuth-film electrode for the determination of trace metals by anodic stripping voltammetry. Int J Electrochem Sci 9:736–759
15. Pham KD, Sohn J-R, Hoeil C (2016) A mechanical pencil lead-supported carbon nanotube/Au nanodendrite structure as an electrochemical sensor for As(III) detection. Analyst 141:5879–5885
16. Vu HD, Pham THY, Nguyen QG, Pham HP, Vu TTH, Pham KD, Hoeil C (2018) A Versatile carbon fiber cloth-supported au nanodendrite sensor for simultaneous determination of Cu(II), Pb(II), and Hg(II). Electroanalysis 30:2222–2227
17. Tran NH, Thothadri G, Kwang SK, Saetbyeol K, Sung-Hwan H, Hoeil C (2011) A three-dimensional gold nanodendrite network porous structure and its application for an electrochemical sensing. Biosens Bioelectron 27:183–186
18. Smith RM, Martell AE, Motekaitis RJ (2004) NIST Critical selected stability constants of metal complexes database. National Institute of Standards and Technology. https://www.nist.gov/sites/default/files/documents/srd/46_8.pdf
19. Zeng A, Liu E, Tan SN, Zhang S, Gao J (2002) Stripping voltammetric analysis of heavy metals at nitrogen doped diamond-like carbon film electrodes. Electroanalysis 14:1294–1298
20. Reeder GS, Heineman WR (1998) Electrochemical characterization of a microfabricated thick-film carbon sensor for trace determination of lead. Sens Actuators, B 52:58–64
21. Gholivand MB, Geravandi B, Parvin MH (2011) Anodic stripping voltammetric determination of iron(II) at a carbon paste electrode modified with dithiodianiline (DTDA) and gold nanoparticles (GNP). Electroanalysis 23:1345–1351
22. Walsh KG, Salaun P, Berg CMG (2011) Determination of manganese and zinc in coastal waters by anodic stripping voltammetry with a vibrating gold microwire electrode. Environ Chem 8:475–484

Affiliations

Nguyen Quynh Giao[1] · Vu Hai Dang[1] · Pham Thi Hai Yen[1] · Pham Hong Phong[1] · Vu Thi Thu Ha[1,2] · Pham Khac Duy[3,4] · Hoeil Chung[4]

[1] Institute of Chemistry, Vietnam Academy of Science and Technology (VAST), 18 Hoang Quoc Viet, Cau Giay, Hanoi, Vietnam

[2] University of Science and Technology of Hanoi, Vietnam Academy of Science and Technology (VAST), 18 Hoang Quoc Viet, Cau Giay, Hanoi, Vietnam

[3] Graduate University of Science and Technology, Vietnam Academy of Science and Technology (VAST), 18 Hoang Quoc Viet, Cau Giay, Hanoi, Vietnam

[4] Department of Chemistry, College of Natural Science, Hanyang University, Seoul, South Korea